

Signal Confidence Limits from a Neural Network Data Analysis¹

Bernd A. Berg^{2,3,4,5} and Jürgen Riedler^{2,4,6,7}

Abstract

This paper deals with a situation of some importance for the analysis of experimental data via Neural Network (NN) or similar devices: Let N data be given, such that $N = N_s + N_b$, where N_s is the number of signals, N_b the number of background events, both unknown. Assume that a NN has been trained, such that it will tag signals with efficiency F_s , ($0 < F_s < 1$) and background data with F_b , ($0 < F_b < 1$). Applying the NN yields N^Y tagged events. We demonstrate that the knowledge of N^Y is sufficient to calculate confidence bounds for the signal likelihood, which have the same statistical interpretation as the Clopper-Pearson bounds for the well-studied case of direct signal observation.

Subsequently, we discuss rigorous bounds for the *a-posteriori* distribution function of the signal probability, as well as for the (closely related) likelihood that there are N_s signals in the data. We compare them with results obtained by starting off with a maximum entropy type assumption for the *a-priori* likelihood that there are N_s signals in the data and applying the Bayesian theorem. Difficulties are encountered with the latter method.

¹This research was partially funded by the Department of Energy under contract DE-FG05-87ER40319 and by the Austrian Ministry of Science.

²Department of Physics, The Florida State University, Tallahassee, FL 32306, USA.

³Supercomputer Computations Research Institute, Tallahassee, FL 32306, USA.

⁴Zentrum für Interdisziplinäre Forschung (ZIF), Wellenberg 1, D-33615 Bielefeld, Germany.

⁵E-mail: berg@hep.fsu.edu

⁶Institut für Kernphysik, Technische Universität Wien, A-1040 Vienna, Austria.

⁷E-mail: juri@kph.tuwien.ac.at

1 Introduction

Let us assume that N_s signals are observed in N data

$$N = N_s + N_b,$$

where N_b is the number of background events. We denote the *a-priori* unknown signal likelihood by p . Relying on the binomial distribution, Clopper and Pearson [1] derived a method, which allows to calculate rigorous confidence bounds on p , given N_s and N . Now, in modern physics, in particular high energy physics experiments, it happens quite often that signal and background events belong to overlapping probability densities in a multi-dimensional parameter space. In such situations signals can only be identified in a statistical sense. Typically, some method may allow to tag signals and background events with different efficiencies: F_s for the signals ($0 < F_s < 1$) and F_b for the background events ($0 < F_b < 1$). Instead of observing N_s signals we only get

$$N^Y \text{ tagged data.}$$

The question is, what confidence limits on the signal likelihood are then implied? We prove, and illustrate in some detail, that the Clopper-Pearson method can be generalized accordingly.

In particular, we have high energy physics experimental data in mind, where tagging may be provided by traditional cuts or by applying some NN [2, 3, 4, 5, 6] technique. To give an example, figure 5 of Ref.[6] depicts values for neural network efficiencies, $F_s(Y)$ and $F_b(Y)$, which one may expect to occur for identifying $t\bar{t}$ -events in the All-Jets channel [7]. Running the network on all N data assigns to each event a value of the network function Y_n , $n = 1, \dots, N$. For a fixed choice of Y , the network returns N^Y events with $Y_n \leq Y$. An additional problem in real applications may be that the efficiencies F_s and F_b are not exact either. However, as outlined in the conclusions, we think that this difficulty may be overcome by the bootstrap approach [8].

In the next section we explain and generalize the Clopper-Pearson approach. A number of illustrations focus on the small number of $N = 10$ data, because then the statistical meaning of the confidence bounds becomes most transparent. In section 3 we deal with the limit of a small number of signals hidden in a large data set. Two instructive sets of network efficiencies are chosen, to demonstrate how the general equations are expected to work in practice.

Section 4 considers *a-posteriori* distribution functions. (i) For the signal probability

$$F(p) = \int_0^p \rho(p') dp'$$

where $\rho(p)$ is the probability density of p . (ii) For the likelihood that there are N_s signals in the data set

$$F(N_s) = \sum_{k=0}^{N_s} P(k),$$

where $P(N_s)$ is the probability that there are N_s signals in the data data. Rigorous lower and upper bounds are provided. For the examples of section 3 those bounds are close together, such that useful approximations of the true *a-posteriori* distribution functions result. In section 5 these results are compared with constructing the $F(N_s)$ distribution function and its $P(N_s)$ probability density with the Bayesian method under the maximum entropy assumption that each N_s is, *a-priori*, equally likely. One of the obtained results, and hence its *a-priori* assumption, is in violation to an exact bound. Conclusions follow in the final section 6.

2 From Neural Network Output to Confidence Limits

Let p be the (unknown) exact likelihood that a data point is a signal. The probability to observe N_s signals within N measurements is given by the binomial probability density

$$b(N_s|N, p) = \binom{N}{N_s} p^{N_s} q^{N-N_s}, \quad q = 1 - p. \quad (1)$$

We are faced with the inverse problem: if N_s signals are observed, what is the confidence to rule out certain p ? Assume that probabilities p_-^c and p_+^c are given. Clopper and Pearson [1] define corresponding lower p_- and upper p_+ bounds as solutions of the equations

$$p_-^c = \sum_{k=N_s}^N b(k|N, p_-) \quad \text{and} \quad p_+^c = \sum_{k=0}^{N_s} b(k|N, p_+) \quad (2)$$

with the additional convention $p_- = 0$ for $N_s = 0$ and $p_+ = 1$ for $N_s = N$. Figure 1 illustrates, how p_- and p_+ are obtained as parameters of the binomial distributions which yield the areas p_-^c and p_+^c as indicated. For this figure we have chosen $N = 26k$ and $N_s = 130$, in the ballpark of values which will interest us in the next section. Here and in the following binomial coefficients have been calculated relying on Fortran routines of [9].

The precise meaning of the bounds (2) is as follows: p_- is the largest number such that (for every feasible p) the probability for $p < p_-$ is less than p_-^c . Correspondingly, p_+ is the smallest number such that the probability for $p > p_+$ is less than p_+^c . The other way round,

$$p \geq p_- \quad \text{with likelihood} \quad P_-^c(p) \geq (1 - p_-^c) \quad (2a)$$

and

$$p \leq p_+ \quad \text{with likelihood} \quad P_+^c(p) \geq (1 - p_+^c). \quad (2b)$$

Therefore, for $p_- < p_+$ we find

$$p \in [p_-, p_+] \quad \text{with likelihood} \quad P^c(p) = P_-^c + P_+^c - 1 \geq (1 - p_-^c - p_+^c). \quad (2c)$$

It is instructive to illustrate these equations for a small value of N . Choosing $N = 10$ and $p_-^c = p_+^c = 0.159$, the precise p -dependence of P_+^c (2b) and of P^c (2c) is depicted in figure 2. The equality $P_+^c(p) = 1 - p_+^c$ is assumed at the discrete values $p = p_+(N_s)$, $N_s = 0, 1, \dots, N$. For example, as long as $p \leq p_+(0)$ holds, p certainty will be smaller than any p_+ bound. As p passes through $p_+(0)$, the probability $P_+(p)$ jumps down to the value $1 - p_+^c = 0.841$. Subsequently $P_+^c(p)$ rises with p in the range $p_+(0) < p < p_+(1)$ until, at $p = p_+(1)$, the next jump occurs, and so on. The corresponding graph for $P_-^c(p)$ follows from $P_+^c(p)$ by reflection

on the $p = 0.5$ axis. The lower, full curve of figure 2 is obtained by combining both according to eqn.(2c).

We are interested in the more involved situation where signal and background can no longer be distinguished unambiguously. Instead, a neural network or similar device yields statistical information by tagging signals with efficiency F_s and background data with efficiency F_b ($0 \leq F_b \leq 1$, $0 \leq F_s \leq 1$ and, typically, $F_b \ll F_s$). Applying the network to all N data results in N^Y , ($0 \leq N^Y \leq N$) tagged data, composed of $N^Y = N_s^Y + N_b^Y$, where N_s^Y are the tagged signals and N_b^Y are the tagged background data. Of course, the values for N_s^Y and N_b^Y are not known. Our task is to determine confidence levels for the signal likelihood p from the sole knowledge of N^Y . We proceed by writing down the probability density of N^Y for given p and, subsequently, generalizing the Clopper-Pearson method.

First, assume fixed N_s . The probability densities of N_s^Y and N_b^Y are binomial and thus the probability density for N^Y is given by the convolution

$$P(N^Y|N_s) = \sum_{N_s^Y + N_b^Y = N^Y} b(N_s^Y|N_s, F_s) b(N_b^Y|N_b, F_b), \quad N_b = N - N_s. \quad (3)$$

Summing over N_s removes the constraint and the N^Y -probability density, with N , p fixed, is

$$P(N^Y|N, p) = \sum_{N_s=0}^N b(N_s|N, p) P(N^Y|N_s). \quad (4)$$

For given p_-^c , p_+^c and N^Y , we define confidence limits p_- and p_+ in analogy with equation (2)

$$p_-^c = \sum_{k=N^Y}^N P(k|N, p_-) \quad \text{and} \quad p_+^c = \sum_{k=0}^{N^Y} P(k|N, p_+). \quad (5)$$

Their meaning is as already outlined by equations (2a-2c). Choosing $F_s = 0.9$, $F_b = 0.2$ and the other parameters as before, figure 3 illustrates these equations for the new situation. The interpretation is as for figure 2 with two remarkable exceptions:

- (i) It may happen that eqn.(5) has no solutions $p_-(N^Y)$ for certain $N^Y = N, N - 1, \dots$ or no solutions $p_+(N^Y)$ for certain $N^Y = 0, 1, \dots$. The reason is that, due to the NN, the result is sufficiently unlikely for all p . One may then either decrease p_-^c or p_+^c or

discard the entire analysis. The parameter values of figure 3 are chosen such that there is no solution $p_+(0)$. Consequently, there is no longer a range of small p -values with $P_+^c(p) = 1$. Such exotic NN output (here $N^Y = 0$) is by definition rare.

- (ii) For $F_s + F_b \neq 1$, the function $P_-^c(p)$ is no longer a reflection of $P_+^c(p)$. This is shown in figure 3, where $P^c(p)$ turns out to be no longer symmetric. In fact, on the r.h.s of figure 3 we observe the same feature as in figure 2: The upper and lower curves agree due to $P_-(p) = 1$ in this range.

In summary, the bounds $[p_-, p_+]$ obtained with $p_-^c = p_+^c = 0.159$ guarantee the standard one error bar confidence probability of 68.2% for every single p -value and for almost all p the actual confidence will be better. However, the one-sided bounds cannot be improved without violating the requested confidence probability for some p -values. In the same way, bounds calculated with $p_-^c = p_+^c = 0.023$ ensure the standard two error bar confidence level of 95.4% or better, and so on. It should be noted that, for $p \neq 0$ and $p \neq 1$, the deviations from the requested confidence probabilities tend to decrease in the limit of large statistics.

3 Large Data Sets with Few Signals

We now assume the values of figure 1 to demonstrate the approach in a limit which is of particular interest for experimental high energy physics applications. With $N = 26k$ and $N_s = 130$ one gets the Clopper-Pearson confidence limits

$$0.00456 \leq p \leq 0.00547 \text{ for } p_-^c = p_+^c = 0.159 ,$$

$$0.00416 \leq p \leq 0.00595 \text{ for } p_-^c = p_+^c = 0.023 .$$

Next, we assume that the only information about the signals is provided by some NN output, where we use two sets of efficiencies, inspired by [6].

First, we consider $F_s = 0.5$ and $F_b = 0.005$. Figure 4 depicts the tag probability density $P(N^Y | N_s)$, see (3), for three different values of N_s : 0, 130 and 260. There is almost no overlap

and, consequently, we expect that clear identification of a positive signal can be achieved. For $N_s = 130$ the central N^Y values are located around $N_s F_s + N_b F_b = 130 F_s + (26000 - 130) F_b = 194.35$. Using $N^Y = 194$, iteration of equation (5) yields the confidence limits

$$0.00389 \leq p \leq 0.00613 \text{ for } p_-^c = p_+^c = 0.159,$$

$$0.00289 \leq p \leq 0.00729 \text{ for } p_-^c = p_+^c = 0.023.$$

The computational demand for these results was less than two hours of CPU time on a DEC 3000 Alpha 600 workstation, where it is important to store frequently used coefficients in RAM.

Let us reduce the signal efficiency to $F_s = 0.1$ and keep the background (in)efficiency unchanged. Figure 5 depicts the new tag probability densities. We find considerable overlap and expect that $p = 0$ can no longer be excluded. The central N^Y values are now located around 142.35. Using $N^Y = 142$, iteration of equation (5) gives

$$0.00005 \leq p \leq 0.010 \text{ for } p_-^c = p_+^c = 0.159,$$

$$0.00000 \leq p \leq 0.0153 \text{ for } p_-^c = p_+^c = 0.023.$$

The latter case should be supplemented by the explicit probability for $p = 0$, estimated in the next section.

4 Signal Probability Distributions

Equation (5), or of course (2) when applicable, can be used to sandwich the *a-posteriori* signal probability distribution $F(p) = F(p|N, N^Y)$ between lower and upper bounds. Namely, it is easy to see that

$$F_1(p) = 1 - p_+^c(p) = \sum_{k=N^Y+1}^N P(k|N, p) \leq F(p) \leq F_2(p) = p_-^c(p) = \sum_{k=N^Y}^N P(k|N, p). \quad (6)$$

For their numerical evaluation the sums should be re-written as $F_2 = 1 - \sum_{k=0}^{N^Y-1} P(k|N, p)$ and $F_1 = F_2 - P(N^Y|N, p)$. Figure 6 depicts these functions for the previously discussed examples $N^Y = 142$ and 194 . Upper and lower bounds are seen close together, such that $F(p) = (F_1(p) + F_2(p))/2$ would be a reasonable working approximation. The corresponding probability densities are the derivatives with respect to p . Their numerical calculation is straightforward when analytical expressions for the derivatives of the binomial coefficients in equation (4) are used. Figure 7 exhibits the results, $P_1(p|N, N^Y)$ and $P_2(p|N, N^Y)$. At $p = 0$ the probability densities have δ -function contributions

$$P_i(p) = F_i(0) \delta(p) + \dots, \quad (i = 1, 2) \quad \text{with} \quad F_1(0) = 0.136 \quad \text{and} \quad F_2(0) = 0.156.$$

In addition, or alternatively to the outlined approach, one may be interested to find for $N_s = 0, 1, \dots, N$ the probabilities that there are N_s signals in the data. That could be done using the probability densities $P_i(p|N, N^Y)$, ($i = 1, 2$), but a calculation starting off from $P(N^Y|N_s)$, equation (3), is far more direct. In particular, it may sometimes be of advantage that N_s , in contrast to p , is a discrete variable. Let us now denote the probability distribution for signals by $F(N_s) = F(N_s|N^Y)$. Lower and upper bounds are

$$F_1(N_s) = \sum_{k=N^Y+1}^N P(k|N_s) \leq F(N_s) \leq F_2(N_s) = \sum_{k=N^Y}^N P(k|N_s). \quad (7)$$

Despite of using the same symbols F , F_1 and F_2 , the functions in equation (6) and (7) are, of course, different. By definition, $F_2(N_s)$ is the likelihood that N_s signals could have produced the observed N^Y or a greater one. Therefore, the likelihood that either of $k = 0, 1, \dots, N_s$ is correct is less or equal the value $F_2(N_s)$, *i.e.* $F_2(N_s)$ is an upper bound of the *a-posteriori* distribution function $F(N_s)$. Similarly, $1 - F_1(N_s)$ is an upper bound on the likelihood that either of $k = N_s, N_s + 1, \dots, N$ is correct. Consequently, $F_1(N_s)$ is a lower bound of $F(N_s)$. Figure 8 depicts theses bounds for our standard examples $N^Y = 142$ and 194 . The similarity with figure 6 is no coincidence, as p determines N_s up to fluctuations of order $1/\sqrt{N}$. Probability densities $P_i(N_s|N^Y)$ are defined by

$$F_i(N_s|N^Y) = \sum_{k=0}^{N_s} P_i(k|N^Y), \quad (i = 1, 2).$$

Defining $F_i(-1) = 0$, they follow recursively

$$P_i(N_s|N^Y) = F_i(N_s) - F_i(N_s - 1), \quad (N_s = 0, 1, \dots, N). \quad (8)$$

Figure 9 exhibits the results. Once the probability densities $P_i(N_s|N^Y)$, $\sum_{N_s=0}^N P_i(N_s|N^Y) = 1$ are known, confidence limits can also be calculated from the subsequent generalization of the Clopper-Pearson (2) approach:

$$p_-^c = \sum_{N_s=0}^N P_2(N_s|N^Y) \sum_{k=N_s}^N b(k|N, p_-), \quad p_+^c = \sum_{N_s=0}^N P_1(N_s|N^Y) \sum_{k=0}^{N_s} b(k|N, p_+). \quad (9)$$

These equations involve nothing, but weighting the binomial Clopper-Pearson sums with the appropriate probabilities $P(N_s|N^Y)$. They re-produce the bounds (5) identically, as was numerically checked for our examples of section 3.

5 Bayesian Approach

Our construction invokes the *a-priori* known fact that the number of signals is in the range $0 \leq N_s \leq N$. It is popular (for reviews see [10, 11]), and sometimes quite successful, to make additional assumptions in form of *a-priori* likelihoods. This can be motivated by a look at figures 2 and 3. For almost all p the confidence is better than the desired 68.2%. If an *a-priori* likelihood is known, the Bayesian approach yields a confidence of precisely 68.2%. The debate is about using *a-priori* likelihoods in situations where they are *not* known. Reasonable guesses can apparently be made in many situations. However, false results are obtained when such a guess is in contradiction with the data, which may not always be trivial to uncover. An example is given here.

In our situation, one would be tempted to impose an *a-priori* likelihood on either p or N_s . For instance, invoking the maximum-entropy principle [12] leads to constant *a-priori* probability densities

$$\rho^0(p) = 1 \quad \text{or} \quad P^0(N_s) = \frac{1}{N+1} \quad \text{for} \quad 0 \leq N_s \leq N. \quad (10)$$

For simplicity we focus on the latter case. (Using the result from [13] it would also be straightforward to work out the other one.) As before, N^Y is determined by measurements and NN analysis. Under the assumption (10) for $P^0(N_s)$, the Bayesian theorem implies the *a-posteriori* probability

$$P(N_s|N^Y) = \text{const. } P(N^Y|N_s), \quad (11)$$

with $P(N^Y|N_s)$ given by equation (3) and the constant follows from the normalization $\sum_{N_s=0}^N P(N_s|N^Y) = 1$. In case of $N^Y = 194$ the result agrees very well with that depicted in figure 9. However, this is not true for $N^Y = 142$, see figure 10, where the probability density of figure 9 is compared with the Bayesian result.

Whereas for strong signal identification the difference with our approach is practically negligible, it is significant for weak (or no) signal identification. The Bayesian probability for $p = 0$ is only 0.00215, implying that the Bayesian distribution function violates the rigorous $F_1(N_s)$ bound. The reason is obvious: It is not clear what *a-priori* probability one should assign to the situation that there is no effect at all. That is why $N_s = 0$ does not compete on the same level as the numbers $N_s \geq 1$. For one of the the situations, we have in mind, no effect at all would mean that there is no top quark. One could assign a finite *a-priori* probability to this possibility, but whether this is 10%, 50% or 90% would be highly arbitrary. Actually it does not even work: As the top quark has already be found [7], one may argue in favor of the given *a-priori* likelihood with the argument that the $N_s = 0$ is certainly very small. However, this leads to an overestimation of large signal probabilities, as the *a-posteriori* $N_s = 0$ likelihood becomes incorrectly re-distributed.

6 Conclusions

We have calculated confidence limits of an unknown signal likelihood for the situation where few signals occur in a large number of events. The only input used were neural network efficiencies for tagging signal and background events as well as the number of data the

network selects. The extension of our approach from the binomial to the multinomial case, *i.e.* to more than two different types of data (signal and background) is certainly possible.

In typical applications the efficiencies F_s and F_b may not be known exactly either. Instead, a number of training sets ($j = 1, \dots, J$) may exist, each giving somewhat different efficiencies F_s^j, F_b^j . We think that in this situation a bootstrap type of approach [8] can be applied and that the probability density (8) provides a suitable starting point. We can linearly combine different probability densities to an ultimate one

$$P_i(N_s) = J^{-1} \sum_{j=1}^J P_i^j(N_s | N_j^Y), (i = 1, 2),$$

and proceed with $P_i(N_s)$ as discussed in section 4.

Finally, to involve conjectured *a-priori* likelihoods may in many situations be unavoidable and, actually, be quite successful. In our case: When a clear, positive signal identification is possible, we find practically no difference between a Bayesian maximum entropy and our approach. However, our example of weak signal identification shows that *a-priori* likelihoods are better avoided when a rigorous alternative exists.

References

- [1] C.J. Clopper and E.S. Pearson, *Biometrika* 26 (1934) 404; S. Brandt, *Statistical and Computational Methods in Data Analysis* (North-Holland, 1983).
- [2] L. Lönnblad, C. Peterson and T. Rönngvaldsson, *Comp. Phys. Commun.* 81 (1994) 187; *Nucl. Phys. B* 349 (1991) 675.
- [3] K.H. Becks, F. Block, J. Dress, P. Langefeld and F. Seidel, *Nucl. Instrum. Methods A* 329 (1993) 501.
- [4] G. Stimpf-Abele and P. Yepes, *Comp. Phys. Commun.* 78 (1993) 1.
- [5] M.D. Richard and R.P. Lippmann, *Neural Comput.* 3 (1991) 461.

- [6] B.A. Berg, *Comp. Phys. Commun.* 98 (1996) 35.
- [7] CDF Collaboration, F. Abe et al., *Phys. Rev. Lett.* 74 (1995) 2626; D0 Collaboration, S. Abachi et al., *Phys. Rev. Lett.* 74 (1995) 2632.
- [8] B. Efron, *J. Am. Stat. Assoc.* 82 (1987) 171.
- [9] W.H. Press, B.P. Flannery, S.A. Teukolsky and W.T. Vetterling, *Numerical Recipes* (Cambridge University Press, 1988).
- [10] T.J. Loredo, *From Laplace to Supernova SN1987A: Bayesian Inference in Astrophysics*, in: *Maximum Entropy and Bayesian Methods*, P.F. Fougère, ed. (Kluwer Academic Publishers, Dordrecht, 1990) pp. 81-142.
- [11] A. Gelman, J. B. Carlin, H.S. Stern and D.B. Rubin, *Bayesian Data Analysis* (Chapman & Hall, 1995).
- [12] E.T. Jaynes, *Proc. IEEE* 70 (1982) 939.
- [13] Ref.[11], p.29.

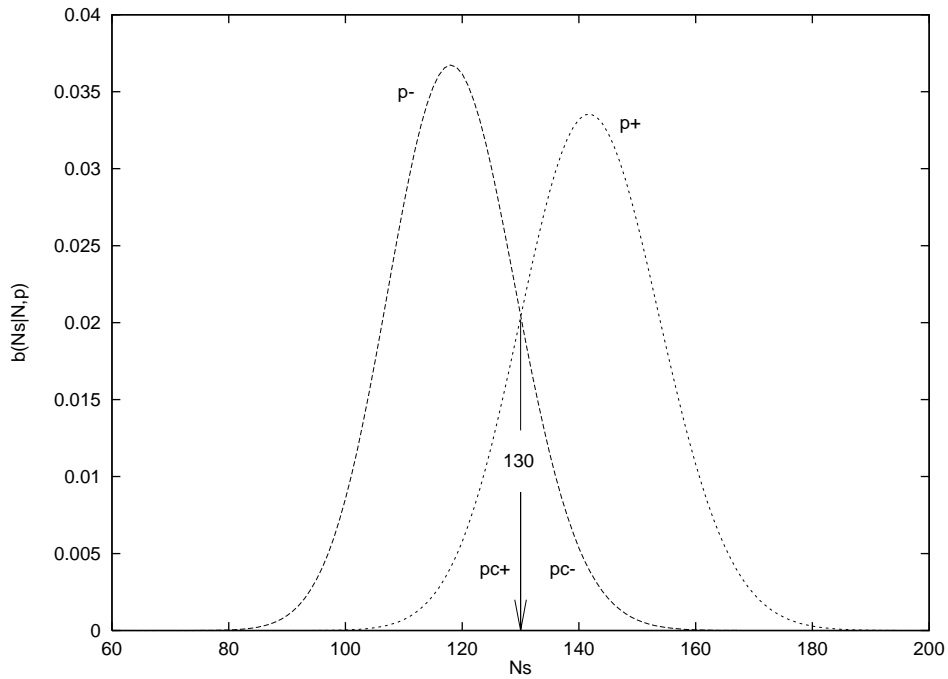


Figure 1: Binomial probability densities corresponding to solving equations (2) for p_+ and p_- with $p_-^c = p_+^c = 0.159$, $N = 26k$ and $N_s = 130$.

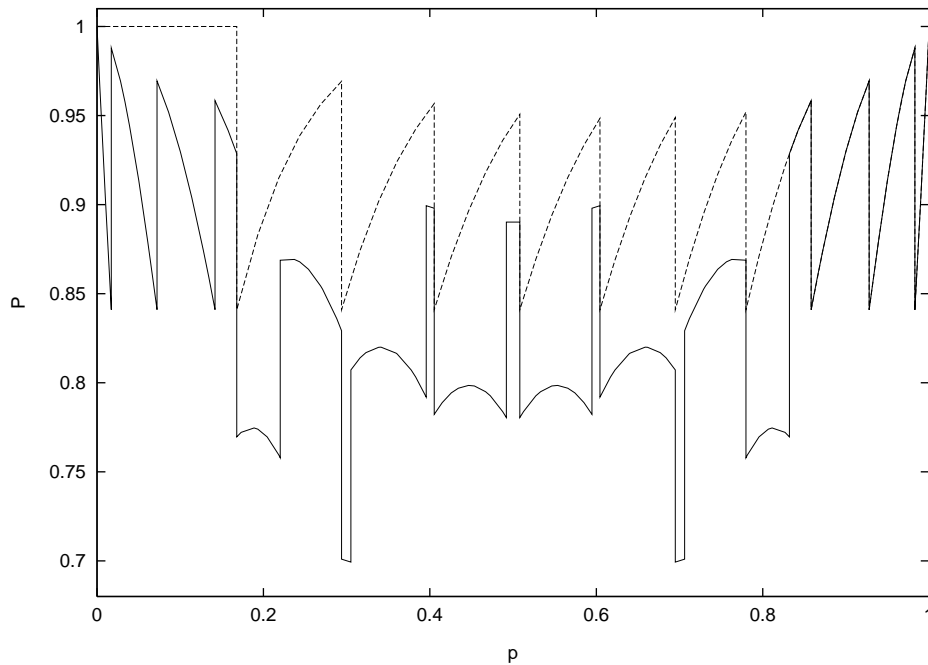


Figure 2: Confidence likelihoods for the Clopper-Pearson bounds (2). The parameters $N = 10$ and $p_-^c = p_+^c = 0.159$ are used. Upper, broken line: Confidence likelihood $P = P_+^c(p)$ (2b) versus the true signal probability p . Lower, full line: Confidence likelihood $P = P^c(p)$ (2c) versus p .

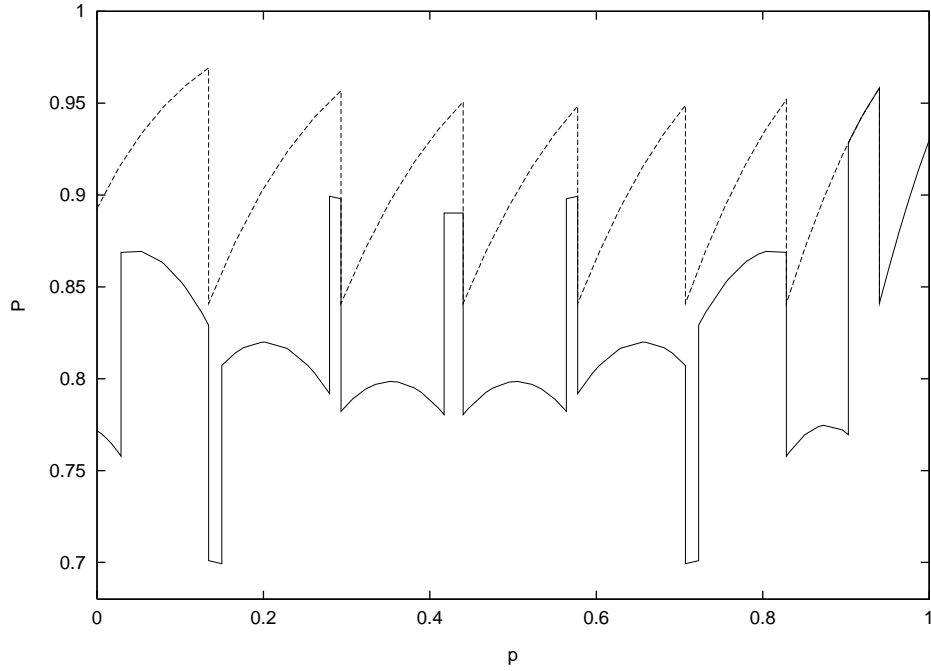


Figure 3: Confidence likelihoods for the generalized Clopper-Pearson bounds (5). The parameters $F_s = 0.9$, $F_b = 0.2$ and those of figure 2 are used. Upper, broken line: Confidence likelihood $P = P_+(p)$ (2b) versus the true signal probability p . Lower, full line: Confidence likelihood $P = P^c(p)$ (5c) versus p .

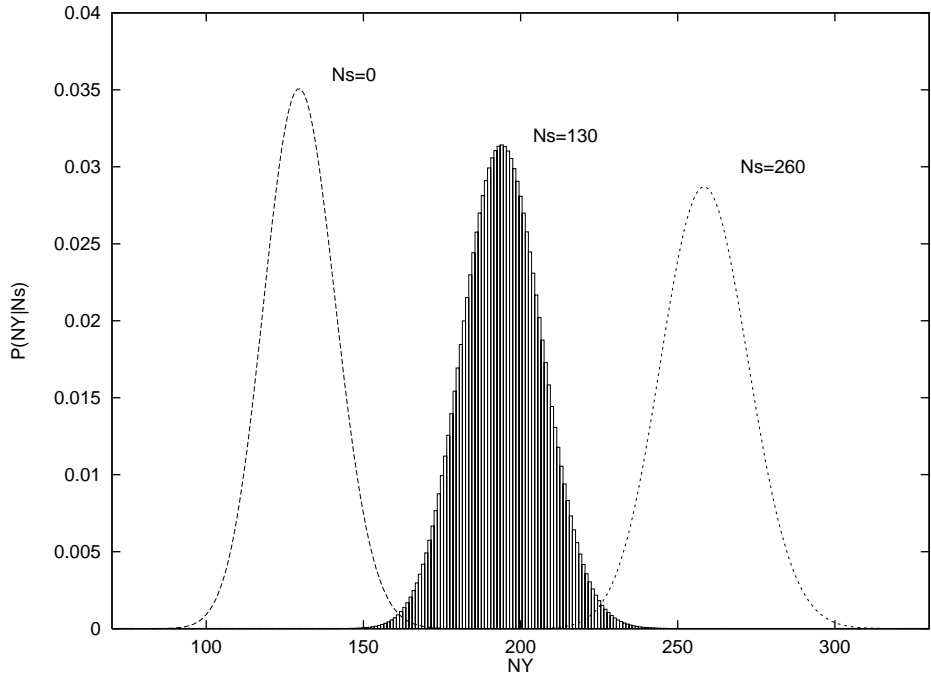


Figure 4: Probability densities to get N^Y data from the NN employing the efficiencies $F_b = 0.005$, $F_s = 0.5$ and assuming N_s signals in the original $26k$ data set.

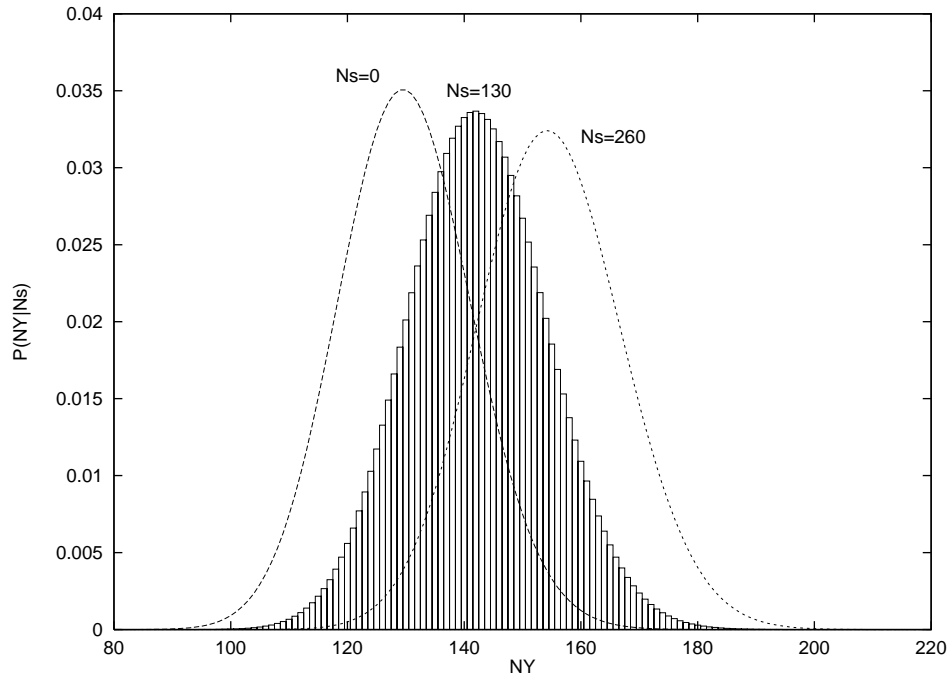


Figure 5: As figure 4, but with signal network efficiency $F_s = 0.1$.

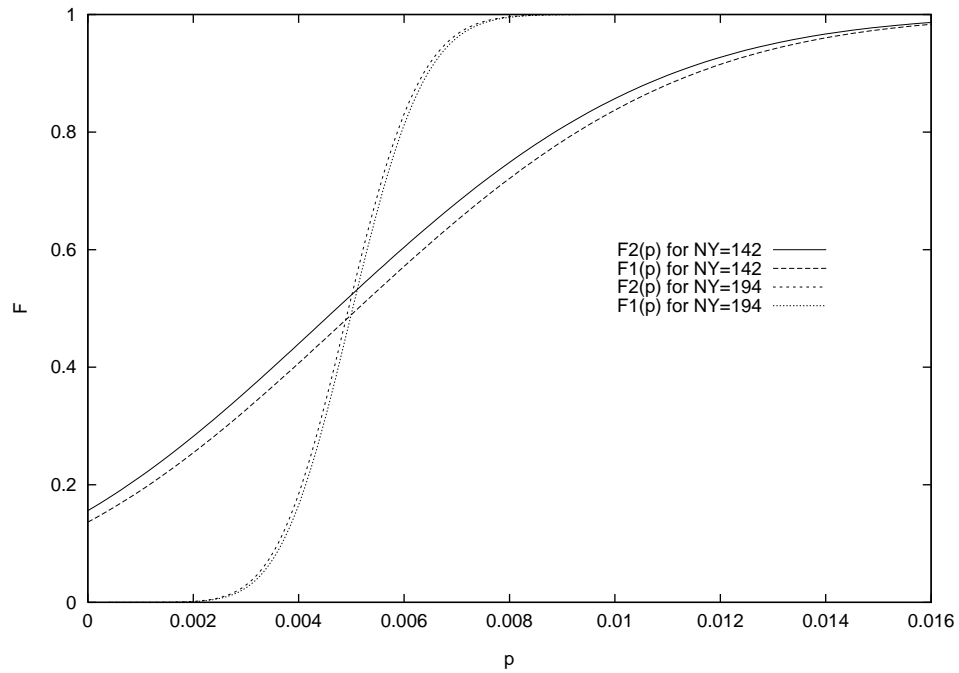


Figure 6: *A-posteriori* signal probability distributions (upper and lower bounds).

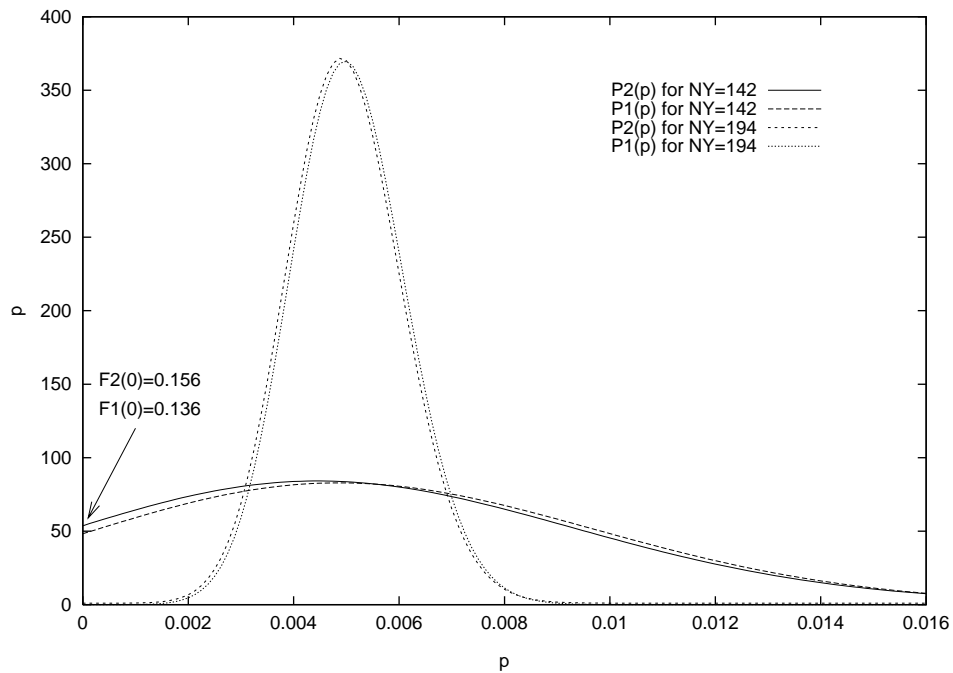


Figure 7: *A-posteriori* signal probability densities (corresponding to upper and lower bounds of the distribution functions in figure 6).

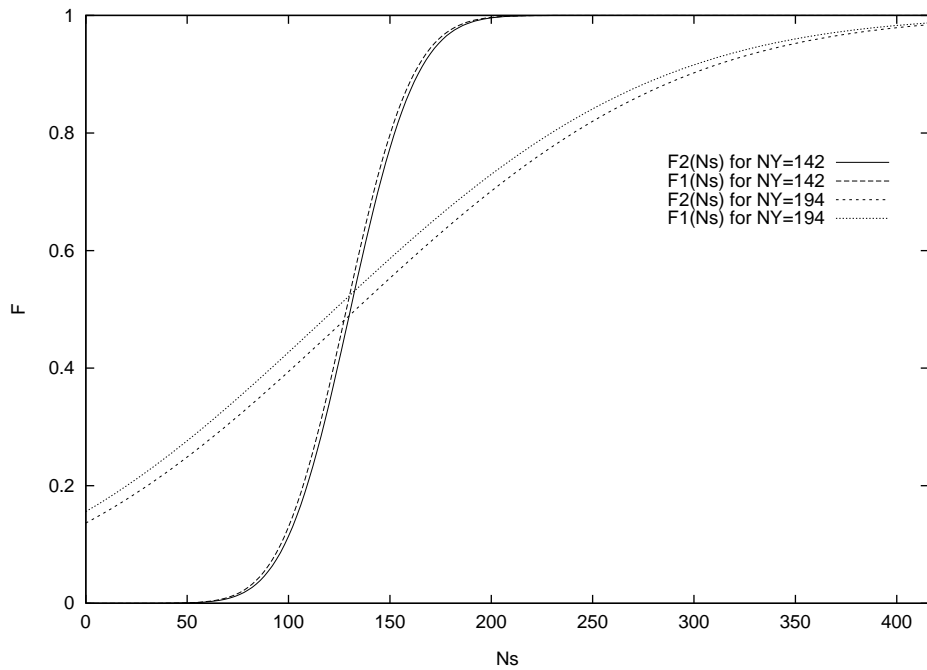


Figure 8: *A-posteriori* distributions for the number of signals (upper and lower bounds).

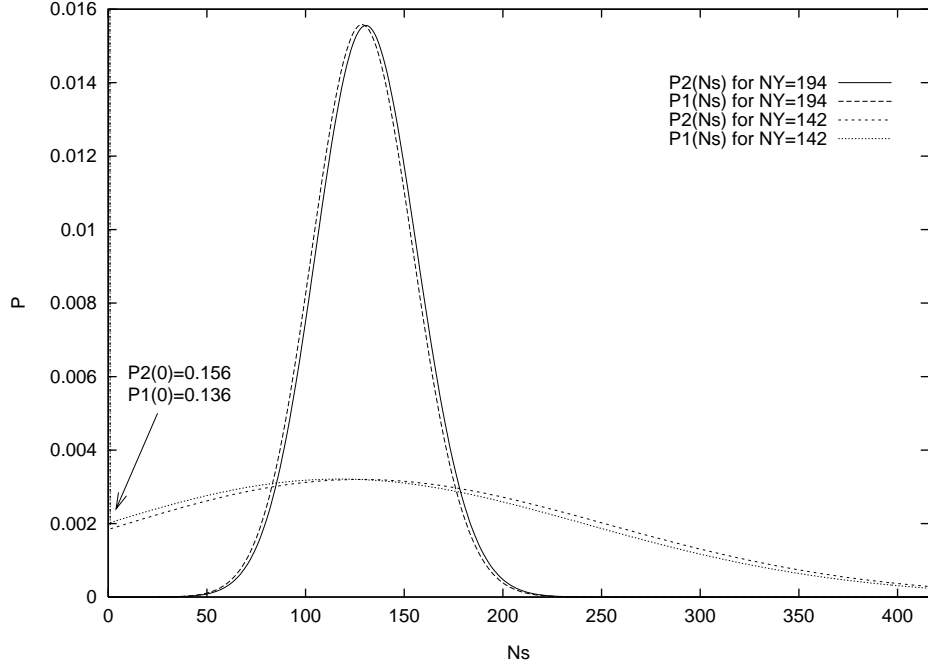


Figure 9: *A-posteriori* probability densities for the number of signals (corresponding to upper and lower bounds of the distribution functions in figure 8).

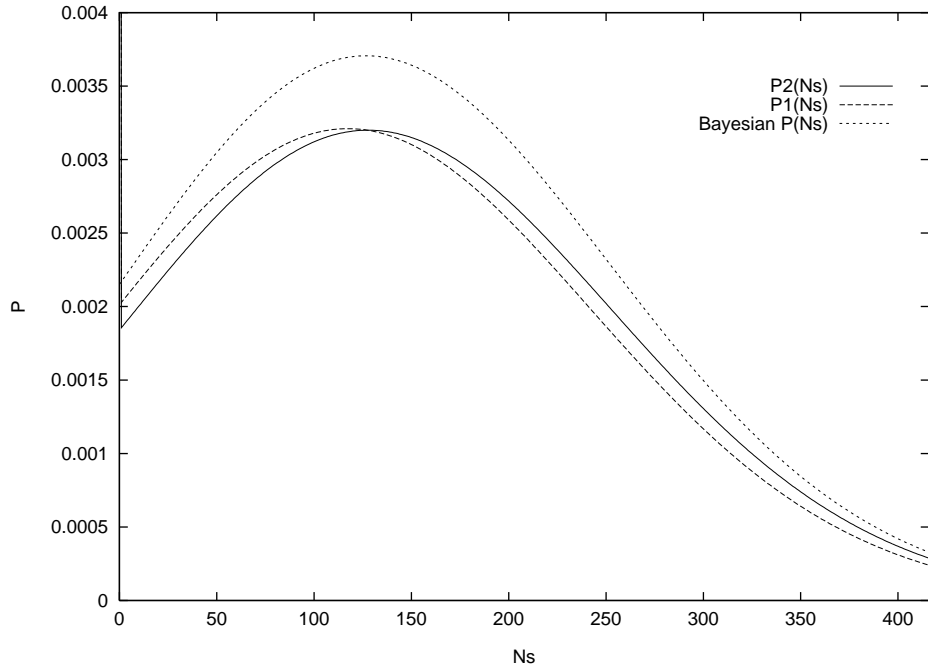


Figure 10: $N^Y = 142$: Comparison of the Bayesian (maximum entropy) *a-posteriori* probability density $P(N_s)$ with $P_1(N_s)$ and $P_2(N_s)$ of figure 9.

